Probing the QCD phase transition with hadron multiplicity ratios

T Bumnedpan[1], J Steinheimer[2], M Bleicher[3,4,5], A Limphirat[1] and C Herold[1]

[1] Center of Excellence in High Energy Physics & Astrophysics, Suranaree University of Technology, Nakhon Ratchasima, 30000, Thailand

[2] Frankfurt Institute for Advanced Studies, Ruth-Moufang-Str. 1, 60438 Frankfurt am Main, Germany

[3] Institut für Theoretische Physik, Goethe Universität Frankfurt, Max-von-Laue-Strasse 1, Frankfurt am Main, 60438, Germany

[4] Helmholtz Research Academy Hesse for FAIR (HFHF), GSI Helmholtz Center for Heavy Ion Physics, Campus Frankfurt, Max-von-Laue-Str. 12, Frankfurt, 60438, Germany

[5] GSI Helmholtzzentrum für Schwerionenforschung GmbH, Planckstr. 1, Darmstadt, 64291, Germany

Email: herold@g.sut.ac.th

Abstract. We investigate the impact of a first-order chiral phase transition and critical point on hadron multiplicity ratios. We model the dynamical expansion of the hot and dense matter created in a heavy ion collision with a Bjorken hydrodynamics expansion coupled to the explicit evolution of the chiral order parameter at center-of-mass energies from 2 to 7 GeV. Hereby, the chiral dynamics is implemented using a Langevin equation including dissipation and noise. We find a strong enhancement of the entropy-per-baryon S/A at lowest energies which is created at the non-equilibrium first-order phase transition. By mapping the initial and final S/A to a hadron resonance gas, we can quantify the shift of hadron multiplicity ratios.

1. Introduction

The main goals of heavy-ion collision experiment are to create and probe a new state of matter called quark-gluon-plasma (QGP) which can be created by a collision at sufficiently large center-of-mass energies [1]. The QGP is a phase where quarks and gluons are deconfined and chiral symmetry is restored. The lattice quantum chromodynamics (QCD) method has been used to identify a crossover transition at small value of baryochemical potential μB. A first-order phase transition and critical end point (CEP) are expected at high baryon density (baryochemical potential) with the CEP location estimated from first principles and effective models [2,3,4].

In experiments, the QCD phase diagram is investigated by measuring cumulant ratios of baryon number, strangeness, and electric charge, e.g., in the beam energy scan program at STAR [5], at NA49/61 [6,7], and HADES [8]. These cumulants are sensitive to the correlation length, so it is still unclear how much of the potential signal survives the non-equilibrium dynamics, finite size and finite time effects. In contrast to that, the non-equilibrium dynamics can be beneficial when considering signals for a first-order phase transition. Due to the delayed relaxation of the critical mode, additional entropy is produced [10], potentially doubling the value (S/A) from the initial state [11].

In this work, we are going to show the effect of additional entropy production on the pion-to-proton multiplicity ratio. We will start with the evolution of the chiral order parameter via a Bjorken hydrodynamics expansion, realistic initial conditions are obtained from the stationary Taub adiabat model [12,13]. We observe differences between an isentropic evolution and the full non-equilibrium dynamics near the CEP and across the first-order phase transition. After a comparison for obtaining the final S/A, we use two parametrized freeze-out curves to map S/A to pion and proton multiplicities using a hadron resonance gas model [14].

2. Model description

To describe the entropy production due to a non-equilibrium first-order chiral phase, a nonequilibrium chiral fluid dynamics Bjorken expansion is utilized [11]. The model is based on the relaxation of the order parameter that obeys a Langevin equation of motion

$$\ddot{\sigma} + \left(\frac{D}{\tau} + \eta\right)\dot{\sigma} + \frac{\delta\Omega}{\delta\sigma} = \xi \tag{1}$$

Here, the dots above σ denote derivative with respect to the proper time τ. Ω is the mean field grand canonical potential and we set $D = 1$ in the Hubble term of longitudinal expansion. The damping coefficient η is related to the stochastic noise ξ with the relation

$$\langle \xi(t)\xi(t')\rangle = \frac{m_\sigma \eta}{V} coth\left(\frac{m_\sigma}{2T}\right)\delta(t-t') \tag{2}$$

with fireball volume V and the sigma screening mass m_σ which is given by second derivative of Ω with respect to σ at the equilibrium state.

In this study, the mean field potential Ω is obtained from a quark-meson model, as integral of the quark degrees of freedom,

$$\mathcal{L} = \bar{q}\left(i\gamma^\mu \partial_\mu - g\sigma\right)q + \frac{1}{2}\left(\partial_\mu \sigma\right)^2 - U(\sigma), \tag{3}$$

$$U(\sigma) = \frac{\lambda^2}{4}(\sigma^2 - f_\pi^2)^2 - f_\pi m_\pi^2 \sigma + U_0 \tag{4}$$

where we use light quarks $q = (u, d)$ and standard parameters $f_\pi = 93$ MeV, $m_\pi = 138$ MeV, $\lambda^2 = 19.7$. This quark-meson model contains the relevant symmetries and essential degrees of freedom to describe a chiral transition at finite baryon density and it also allows us to solve the proper equation of motion for the chiral field.

We assume that most entropy in the initial state of low-energy heavy ion collisions is produced by compression after the heavy nuclei have collided, which can be described by the Rankine-HugoniotTaub adiabat [12,13],

$$(P_0 + \varepsilon_0)(P + \varepsilon_0)n^2 = (P_0 + \varepsilon)(P + \varepsilon)n_0^2 \tag{5}$$

where $P_0 = 0, \frac{\varepsilon_0}{n_0} - m_N = -16$ MeV and $n_0 = 0.16$ fm^{-3} are the ground state pressure, energy density and baryon density respectively. With any known $P = P(T, \mu_B)$ and $\varepsilon = \varepsilon(T, \mu_B)$, Eq. 5 can be solved. Moreover, the collision energy can be related to the compression as:

$$\gamma^{CM} = \frac{\varepsilon n_0}{\varepsilon_0 n}, \quad \gamma^{CM} = \sqrt{\frac{1}{2}\left(1 + \frac{E_{lab}}{m_N}\right)}. \tag{6}$$

Here, γ^{CM} is the Lorentz gamma factor in the center of mass frame of the heavy ion collisions and E_{lab} is the beam energy per nucleon in the laboratory frame of a fixed target collision.

3. Results

Our simulation starts from initial conditions (5), (6) and then proceeds according to equations (1), (2), until a proper time of 12 fm, yielding trajectories of actual evolutions of temperature and baryochemical potential for each initial condition corresponding to a certain center-of-mass energy.

Figure 1 exhibits trajectories averaged over events for initial conditions at three different center-of-mass energies, along with their corresponding initial values of S/A. The Taub adiabat is represented by the blue line. The solid black curve, along with the adjacent dot at $(T, \mu_B) = (100{,}200)$ MeV, indicates the location of the first-order phase transition and the critical end point of the quark-meson model in mean field. For each initial condition, a comparison is made between non-equilibrium evolutions (solid lines) and isentropic evolution (dashed lines) with constant S/A, serving as an ideal hydrodynamics evolution. These non-equilibrium evolutions are subsequently used as a proxy for scenarios without a first-order phase transition.

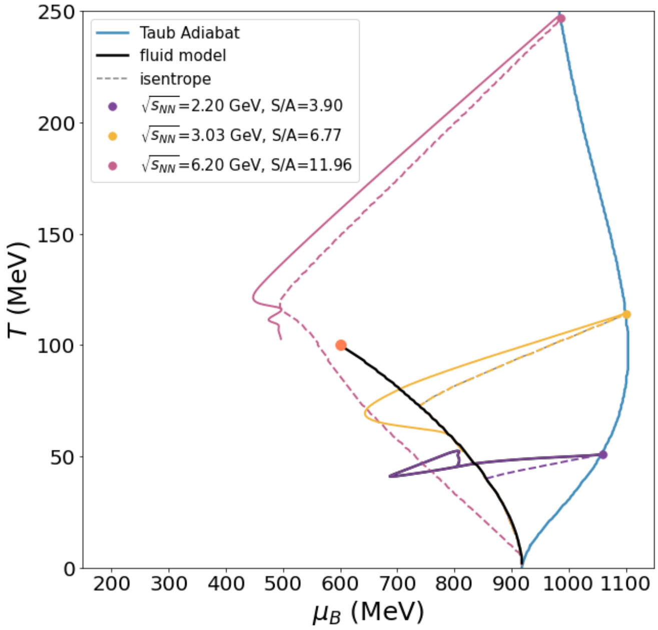

Figure 1: Evolutions of the fluid dynamical model (solid lines) compared to the isentropes (dashed lines) from the same initial condition along the Taub Adiabat. The position of CEP and first-order phase transition are indicated by the dot and solid black line. Figure from [15].

To establish criteria for freeze-out, we analyze two distinct situations. Given the model's emphasis on the sigma field, we utilize its behavior to determine the point at which entropy production stops. First, at a constant value of $\sigma_{f.o.} = 70$ MeV, and second, at the point where the slope in the function $\sigma(\tau)$ remains constant, a signal of transition completion i.e. $d^2\sigma/d\tau^2|_{\sigma=\sigma_{f.o.}} = 0$. Figure 2 displays the chiral order parameter evolutions for the three different initial entropy per baryon values, along with the selected points corresponding to the two criteria.

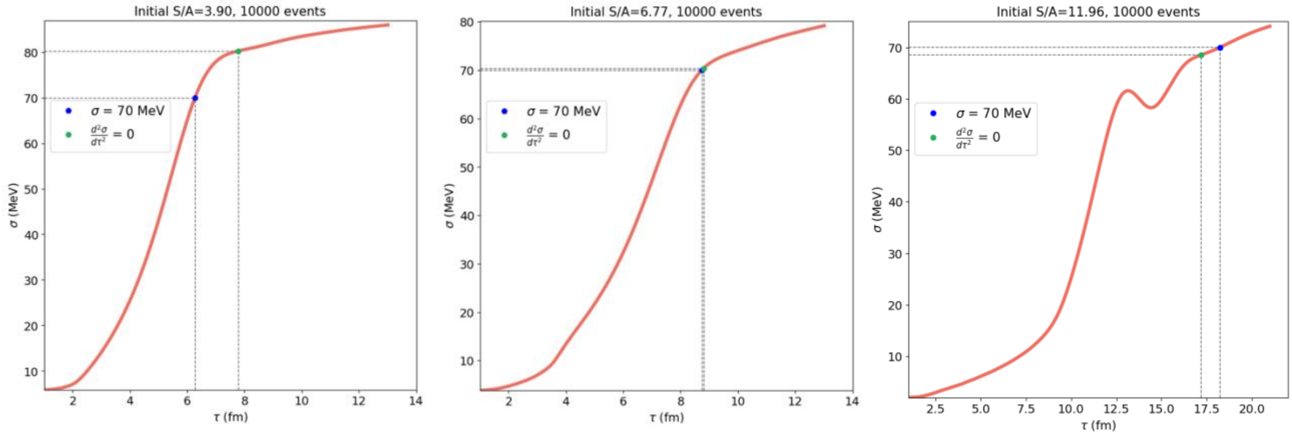

Figure 2: Evolutions of chiral order parameter at different initial entropy per baryon number, averaged over 10^4 events.

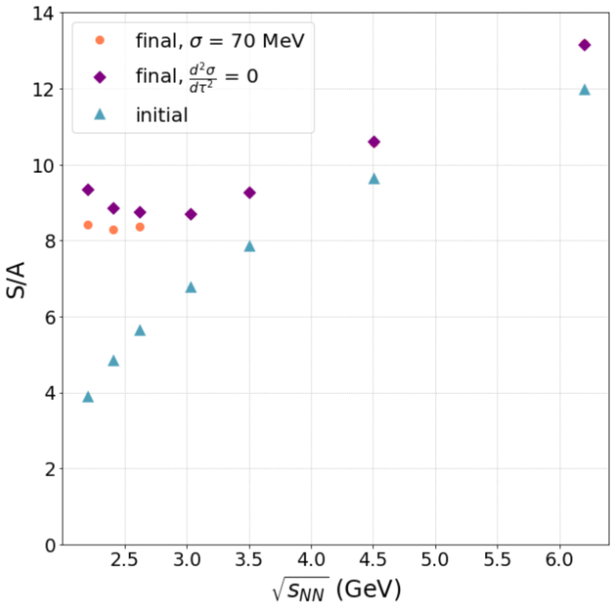

Figure 3: Initial and final entropy-per-baryon number, the latter one extracted for two different freeze-out conditions. In both cases, a clear enhancement at low energies is found compared to the initial value. Figure from [15].

For more clarification, Figure 3 illustrates the final entropy per baryon (S/A) obtained from both selection criteria as a function of the center-of-mass energy $\sqrt{s_{NN}}$ together with the initial S/A, along with the initial S/A values derived from the Taub Adiabat. The plot demonstrates a clear and continuous rise in the initial S/A with increasing energy. Additionally, there is a notable overall improvement in the final S/A values compared to the initial ones, showing a general enhancement as the energy increases. Note that both freeze-out conditions result in final values for S/A that are strongly enhanced at lowest $\sqrt{s_{NN}}$, with only slightly different values. Since both freeze-out conditions yield similar results, we will discuss only the criteria of $d^2\sigma/d\tau^2|_{\sigma=\sigma_{f.o.}} = 0$.

To convert the final state entropy per baryon (S/A) into particle multiplicities, we matched the obtained S/A value to a parametrized freeze-out curve. This was done by identifying T and μ_B along that curve corresponding to the final S/A. With these T and μ_B values, we employed the Thermal-FIST (Thermal, Fast, and Interactive Statistical Toolkit) package [16] to calculate the numbers of pions and protons using a hadron resonance gas model. As there is currently no consensus on the exact location of the freeze-out curve, especially at the lowest energies, we compared results from two different versions obtained from thermal model fits to experimental data covering a wide range of energies using the parametrization

$$T_{f.o.}(\mu_B) = a - b\mu_B^2 - c\mu_B^4 \qquad (7)$$

with parameter set A as $a = 0.157$ GeV, $b = 0.087$ GeV^{-1} and $c = 0.092$ GeV^{-3} (freeze-out curve A [17]) and parameter set B as $a = 0.166$ GeV, $b = 0.139$ GeV^{-1} and $c = 0.053$ GeV^{-3} (freeze-out curve B [18]).

In Figure 4, we can see the ratio of charged pions to protons obtained from the hadron resonance model. The plot presents results for both freeze-out curves A and B, considering scenarios with and without a phase transition. Overall, we observe that the presence of a phase transition (indicated by the cross and square symbols) leads to a noticeable enhancement of the multiplicity ratio compared to the situation without a phase transition (represented by the diamond and circle symbols). This enhancement is particularly prominent at low values of $\sqrt{s_{NN}}$ where the ratio values increase again after initially decreasing at lower energies. Since freeze-out curve A lies above curve B throughout the investigated energy range, the same is true for the corresponding pion-to-proton ratios.

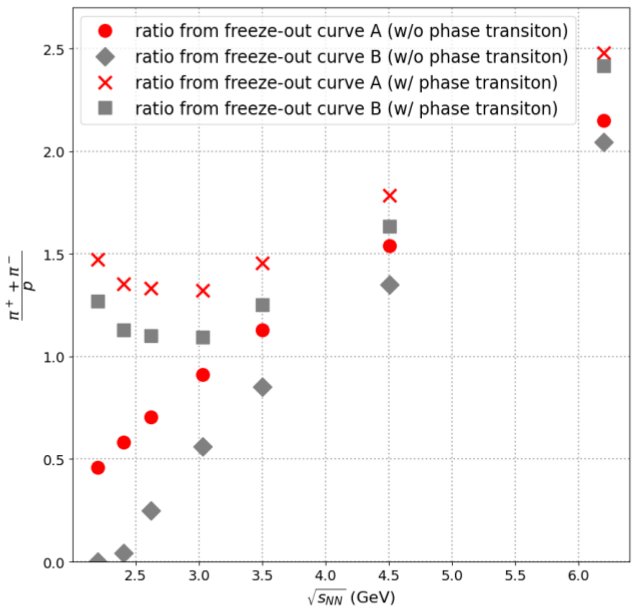

Figure 4: Pion-to-proton multiplicity ratio as function of center-of-mass energy for scenarios with and without phase transition. For both freeze-out curves, we see a strong enhancement at low energies for scenarios with a phase transition. Figure from [15].

4. Summary and conclusions

In our investigation, we have examined the impact of the chiral first-order phase transition on two key quantities: the entropy-per-baryon number and the pion-to-proton ratio. To do this, we coupled a Bjorken expansion with the non-equilibrium evolution of the order parameter. Additionally, we calculated particle multiplicities using two different parametrizations of freeze-out conditions. These parametrizations were obtained from experimental data fitting to the thermal model. By combining these approaches, we aimed to gain insights into the behavior and characteristics of the chiral first-order phase transition and its influence on the mentioned observables.

Compared to a scenario without a phase transition, a non-equilibrium first-order phase transition leads to a significant increase in both S/A and the pion-to-proton ratio. If a QCD phase transition occurs at high baryochemical potentials, experiments should exhibit a sudden jump in the pion-to-proton ratio when a chirally restored phase is created.

References

[1] Adams J, et al. (STAR), Nucl. Phys. A 757 (2005) 102-183. doi: 10.1016/j.nuclphysa.2005.03.085. arXiv:nucl-ex/0501009
[2] Scavenius O, Mocsy A, Mishustin I N, Rischke D H, Phys.Rev. C64 (2001) 045202. doi:10.1103/PhysRevC.64.045202. arXiv:nucl-th/0007030
[3] Schaefer B -J, Wambach J, Nucl.Phys. A757 (2005) 479-492. doi:10.1016/j.nuclphysa.2005.04.012. arXiv:nucl-th/0403039
[4] Fukushima K, Phys.Rev. D77 (2008) 114028. doi:10.1103/PhysRevD.77.114028.10.1103/PhysRevD.78.039902. arXiv:0803.3318
[5] Abdallah M, et al (STAR), Phys. Rev. C 104 (2021) 024902. doi:10.1103/PhysRevC.104.024902. arXiv:2101.12413.
[6] Grebieszkow K (NA49 Collaboration), Nucl.Phys. A830 (2009) 547C-550C. doi:10.1016/j.nuclphysa.2009.09.044. arXiv:0907.4101.
[7] Andronov E (NA61/SHINE), Nucl. Phys. A 982 (2019) 835-838. doi:10.1016/j.nuclphysa.2018.09.019. arXiv:1807.10737
[8] Adamczewsci-Musch J, et al. (HADES), Phys. Rev. C 102 (2020) 024914. doi:10.1103/PhysRevC.102.024914. arXiv:2002.08701.
[9] Karsch F, J. Phys. Conf. Ser. 779 (2017) 012015. doi:10.1088/1742-6596/779/1/012015. arXiv: 1611.01973.
[10] Csernai L P, Kapusta J I, Phys. Rev. Lett. 69 (1992) 737–740. doi:10.1103/PhysRevLett.69.737.
[11] Herold C, Kittiratpattana A, Kobdaj C, Limphirat A, Yan Y, Nahrgang M, Steinheimer J, Bleicher M, Phys. Lett. B 790 (2019) 557–562. doi:10.1016/ j.physletb.2019.02.004. arXiv:1810.02504.
[12] Taub A H, Phys. Rev. 74 (1948) 328–334. doi:10.1103/ PhysRev.74.328.
[13] Thorne K S, Astrophys. J. 179 (1973) 897–908. doi:10. 1086/151927.
[14] Vovchenko V, Stoecker H, Comput. Phys. Commun. 244 (2019) 295–310. doi:10.1016/j.cpc.2019.06.024. arXiv:1901.05249.
[15] Bumnedpan T, Steinheimer J, Bleicher M, Limphirat A, Herold C, Physics Letters B, Volume 835, 2022, 137537, https://doi.org/10.1016/j.physletb.2022.137537.
[16] Vovchenko V, Stoecker H, Comput. Phys. Commun. 244 (2019) 295–310. doi:10.1016/j.cpc.2019.06.024. arXiv:1901.05249.
[17] Vovchenko V, Begun V V, Gorenstein M I, Phys. Rev. C 93 (2016) 064906. doi:10.1103/PhysRevC.93. 064906. arXiv:1512.08025.
[18] Cleymans J, Oeschler H, Redlich K, Wheaton S, Phys. Rev. C 73 (2006) 034905. doi:10.1103/PhysRevC. 73.034905. arXiv:hep-ph/0511094.